A multi-objective optimization problem in mixed and natural convection for a vertical channel asymmetrically heated

Delphine Ramalingom, Pierre-Henri Cocquet, Rezah Maleck, Alain Bastide

A multi-objective optimization problem in natural convection for a vertical channel asymmetrically heated

Delphine Ramalingom[a,*], Pierre-Henri Cocquet[a], Rezah Maleck[a], Alain Bastide[a]

[a] *Université de La Réunion, Laboratoire PIMENT, 117 Avenue du Général Ailleret, 97430 Le Tampon, France*

Abstract

This paper deals with a multi-objective topology optimization problem in an asymmetrically heated channel, considering both pressure drop minimization and heat transfer maximization. The problem is modeled under the assumptions of steady-state laminar flow dominated by natural convection forces. The incompressible Navier-Stokes equations coupled to the convection-diffusion equation through the Boussinesq approximation are employed and are solved with the finite volume method. In this paper, we propose two new objective functions: the first one takes into account work of pressure forces and contributes to the loss of mechanical power while the second one is related to thermal power and is linked to the maximization of heat exchanges. In order to obtain a well-defined fluid-solid interface in the optimized design, we use a sigmoid interpolation function for both the design variable field and the effective diffusivity. We also use adjoint sensitivity analysis to compute the gradient of the cost functional. Results are obtained for various Richardson (Ri) number such that $100 < \mathrm{Ri} < 400$ and

*Corresponding author: delphine.ramalingom@univ-reunion.fr

for a Reynolds (Re) number set to Re = 400. In all considered cases, our algorithm succeeds to enhance one of the phenomenon modeled by our new cost functions without deteriorating the other one. We also show that the reversal flow is suppressed at the exit of the channel, the thermal exchanges are improved by our optimized designs. We also compare the results of standard cost functions from the literature to those of our cost functions. We show that the new objective functions reached stable values in less iteration number and allow best connectivity of solid elements. As a result the new objective functions proposed in this paper are well suited to deal with natural convection optimization problem.
Keywords: Natural convection, Vertical channel, Topology optimization, Objective functions, Adjoint sensitivity analysis, Sigmoid function

Nomenclature

List of abbreviations

b	Channel width
d	Width of circulation flow
g	Gravitational acceleration
h_τ	Ratio between a kinematic viscosity and a permeability
k_τ	Effective diffusivity, dimensionless
p	Pressure, dimensionless
$\mathbf{u}$	Velocity vector, dimensionless
Gr_b	Grashof number
H	Height of heated plate, channel height $A = 2H$
Nu_2	Nusselt number based on θ_b
Pr	Prandtl number
Q_t	Proportion of material added in Ω at the end of optimization process
Ra_b	Rayleigh number based on b
Re	Reynolds number
Ri	Richardson number
T	Fluid temperature
U	Average velocity at the entrance of the channel

$\mathcal{J}$	Objective function
$\mathcal{L}$	Lagrangian function

Greek symbols

α	Design parameter
ν	Kinematic viscosity
Φ	Heat flux at the hot plate
Ω	Computational domain
α_0, τ	Parameters of sigmoid functions
β	Thermal expansion coefficient
γ_1,γ_2	Weighting coefficients
Γ	Frontiers of the domain
Δ	Variation
ϵ	Stopping criterion in optimization algorithm
θ	Temperature, dimensionless
λ_f	Thermal conductivity of fluid

Subscripts

b	bulk
o	outlet
i	inlet
max	maximum value

1. Introduction

Topology optimization is a powerful and a popular tool for designers and engineers to design process. Its notion was initially introduced in structural mechanics by Bendsøe and Kikuchi [1]. In order to increase the structural stiffness under certain load, they targeted the optimal material density distribution by identifying areas in which material should be added. They expressed the design problem in terms of real valued continuous function per point, with values ranging from zero (indicating the presence of void/absence of material) to unity (indicating solid). The method has then been developed to numerous problems in structural mechanics [2, 3, 4, 5, 6, 7, 8]. In fluid mechanics, the same idea was adapted to Stokes flows by Borrvall and Petersson [9], by introducing a real-valued inverse permeability multiplied by a kinematic viscosity dependent term into the flow equations. Domain areas corresponding to the fluid flow are those where α is equal to 0 while areas where α is not equal to 0 define the part of the domain to be solidified. The optimal solid walls to be designed correspond to the interfaces between the two aforementioned areas. So, the goal of topology optimization is to compute the optimal α field in order to minimize some objective function under consideration. Contrary to topology optimization applied to design structure, research on topology optimization applied to heat transfer and fluid dynamics is quite recent. Dbouk [10] presented a review about topology optimization design methods that have been developed for heat transfer systems, and for each of them, he presented their advantages, limitations and perspectives. In topology optimization problems with large number of design variables, gradient-based algorithms are frequently used to compute accurate solutions efficiently [11, 12, 13, 14, 15, 16]. This algorithm starts with a given geometry and iterates with information related to the derivatives (sensitivity derivatives) of the objective function with respect to the design variables. Among the methods used to compute the sensitivity derivatives required by gradient-based methods, the adjoint method [11, 17, 18, 19, 12, 20] has been receiving a lot of attention since the cost of computing the necessary derivatives is independent from the number of design variables. Papoutsis-Kiachagias and Giannakoglou [18] present a review on continuous adjoint method applied to topology optimization for turbulent flows. Tong et al. [21] have recently discussed on the optimization of thermal conductivity distribution for heat conduction enhancement. They considered different optimization objectives and demonstrate that they should be carefully chosen when heat conduction is involved. Othmer [19] derived the continuous adjoint formulations and the boundary conditions on ducted flows for typical cost functions. He proposed an objective function to reduce pressure drops in open cavity. The originality of his method is the versatility of the formulation where the adjoint boundary conditions were expressed in a form that can be adapted to any commonly used objective function. Then, for the automotive industry, Othmer et al. [22] implemented several objective functions like dissipated power, equal mass flow through different outlets and flow uniformity. To describe the transition and interface between fluid and solid regions in the domain, the Solid Isotropic Material with Penalization (SIMP) technique [1, 23] is the mostly used in the literature as the interpolation technique in topology optimization. This approach represents the non-fluid regions as infinitely stiff, a penalty to the flow, such that no interaction is modeled. Yoon [16] presented a method for solving static fluid-structure interaction problems by converting the stresses at the fluid-solid interfaces into a volume integral representation. A new method of interpolation was presented by Ramalingom et al. [24] in order to improve the interface fluid-solid during the optimization process. They proposed two sigmoid functions to interpolate material distribution and effective diffusivity. They showed that transition zones, i.e. zones where the velocity of fluid is too large to be considered as solid, can be made arbitrary small.

Convection typically is categorized, according to fluid motion origins, as forced, mixed or natural [25, 26]. All aforementioned references on heat transfer problems deal with forced or mixed convection. This means that the fluid motion is driven by a fan, pump or pressure gradient often modeled by a non-null velocity at entrance of the studied domain. Although natural convection is often used for the passive cooling of industrial systems, very few studies have been investigated for topology optimization problem in natural convection case. Natural convection involves a heat dissipation mechanism where the fluid motion is governed by differences in buoyancy arising from temperature gradients. More precisely, the fluid is submitted to a small velocity, the corresponding heat rates are also much lower than those associated with forced convection. Coffin and Maute [27] introduced a topology optimization method for 2D and 3D, steady-state and transient heat transfer problems that are dominated by natural convection in the fluid phase. The geometry of the fluid-solid interface is described by an explicit level set method. Alexandersen et al. [13] applied topology optimization to natural convection problems. Its study shows that topology optimization is a viable approach for designing heat sink geometries cooled by natural convection and micropumps powered by natural convection. He treated several difficulties that would be encountered when dealing with natural convection problems as the oscillatory behavior of the solver, namely a damped Newton method, used for the optimization computations. He also reported intermediate relative densities that amplified the natural convection effects leading to non-vanishing velocity in some solid parts of the computational domain. As a result, those zones are considered as solid by the optimization algorithm while they should be treated as fluid. Bruns [15] applied topology optimization to convection-dominated heat transfer problems. He highlighted numerical instabilities in convection-dominated diffusion problems and justified them by the density-design-variable-based topology optimization.

Other numerical issues are encountered in topology optimization problems, as checkerboards pattern and intermediate density regions. Authors usually adopted a continuation strategy where the parameter involved in the SIMP interpolation of the effective diffusivity is gradually increased during the optimization process. These values are chosen to aggressively penalize intermediate densities with respect to effective diffusivity and to confine the maximum impermeability to the fully solid parts of the domain. Similarly, authors used filtering techniques [28, 29, 30, 12, 13] to overcome checkerboards. The filtering is done by looking at the ”neighborhood” of the individual element which is defined as the set of elements with centers within the filter radius. Bruns [29] explained that the main disadvantage of filtering the sensitivities is that the approach is heuristic because the sensitivities are not consistent with the primal analysis. Therefore, the optimization problem is not well posed in a rigorous sense. Alexandersen et al. [31] explained that some form of filtering can be beneficial for some topology optimization problems. Minimizing the dissipate energy in fluid flow problems are generally well posed and no filtering is needed. In contrarily, alternating solid and fluid elements can exist in structural and heat transfer problems. That creates areas of solid elements not correctly connected. Sigmund [32] described various filters type to fix this problem.

In this paper, we deal with some topology optimization problems for heat and mass transfers, considering the physical case of an asymmetrically heated vertical channel. This geometry has been subject to numerous studies in the literature [33, 34, 35, 36]. The first investigations date back to 1942 with the works of Martinelli and Boelter [37] according to the comprehensive review of Jackson et al. [38]. Developing and fully developed laminar free convection within heated vertical plates were subsequently investigated numerically by Bodoia and Osterle [39] and was experienced by Elenbaas [40]. Since then, many studies were carried out. This great interest can be explained by the fact that this configuration is encountered in several industrial devices such as solar chimney, energy collectors, electronic components and even in nuclear reactors. The optimization of these systems simultaneously demands compactness, efficiency and control of heat and mass transfers.

This paper investigates new objective functions to optimize heat transfer in convection-dominated diffusion problems. Instead of proposing methods to improve filtering techniques and avoid some non-physical solutions related in literature [41, 15], we propose new expressions of objective functions within the framework of topology optimization applied to an asymmetrically heated vertical channel. Furthermore, no filtering techniques have been used during the optimization process.The geometry considered here is the model proposed by Desrayaud et al. [42] and corresponds to a boundary layer flow with a reversal flow at the exit [43]. We study the influence of Richardson number, which represents the importance of natural convection relative to the forced convection, in the optimized design. This adimensional number is chosen such as natural convection forces are dominant. Our optimization algorithm succeeds especially to suppress the reversal flow. We show that our optimized design increase thermal exchanges by computing the Nusselt numbers for the range of Richardson numbers considered. We finally compare our results at the end of the optimization process to those obtained with classical objective functions of the literature. We conclude that our expression of cost functions are best suited to the optimization of convection-dominated diffusion problems which agrees closely with Tong et al. [21] about the importance of the choice of objective function in optimization problem.

2. Governing equations

The flows considered in this paper are assumed to be in a steady-state laminar regime, newtonian and incompressible. Figure 1 shows the configuration of the computational domain Ω.

Physical properties of the fluid are kinematic viscosity ν and thermal conductivity λ_f. First, parameters governing the flow is the Reynolds number defined as $\mathrm{Re} = U\ b/\nu$, with b being the width of the channel and U the reference velocity based on the average velocity at the channel entrance. The Prandtl number is defined as $\mathrm{Pr} = \nu/k$. It describes the ratio between the

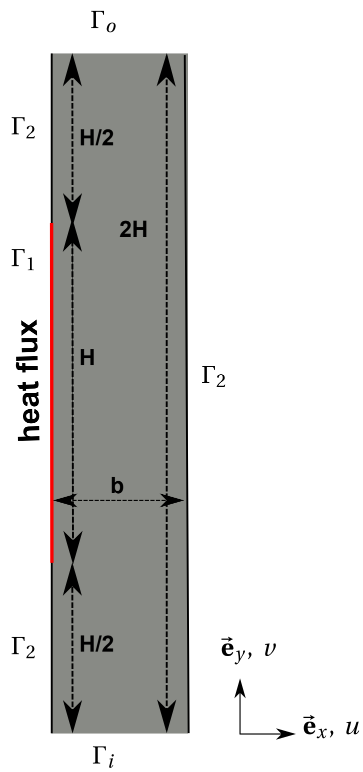

Figure 1: Geometry of the problem

momentum and thermal diffusivities of the fluid. In this paper, we consider only fluids with small Prandtl as $\mathrm{Pr} < 1$. The Grashof number is defined as $\mathrm{Gr}_b = g\ \beta\ \Delta T\ b^3/\nu^2$ and represents the ratio between buoyancy and viscous force. $\Delta T = -\phi/\lambda_f$, ϕ is the thermal flux on Γ_1. In thermal convection problems, Richardson number $\mathrm{Ri} = \mathrm{Gr}_b/\mathrm{Re}^2$ represents the importance of natural convection relative to the forced convection. For values greater than unity, we know that the flow is dominated by natural convection. Under these assumptions and thanks to a method given in Borrvall and Petersson [9], the porosity field is introduced in the steady-state Navier-Stokes equation as a source term $h_\tau(\alpha)\mathbf{u}$ which yields a Brinkman-like model with a convection term [24]. Therefore, the dimensionless form of the Navier-Stokes and energy equations are written as follows:

$$\begin{aligned}
\nabla \cdot \mathbf{u} &= 0 && \text{in } \Omega, \\
(\mathbf{u} \cdot \nabla)\ \mathbf{u} &= -\nabla p + \mathrm{Re}^{-1} \Delta \mathbf{u} - h_\tau(\alpha)\mathbf{u} + \mathrm{Ri}\ \theta\ \overrightarrow{e_y} && \text{in } \Omega, \\
\nabla \cdot (\mathbf{u}\theta) &= \nabla \cdot (\mathrm{Re}^{-1}\mathrm{Pr}^{-1} k_\tau(\alpha)\nabla\theta) && \text{in } \Omega,
\end{aligned} \tag{1}$$

where $(\mathbf{u}, p, \theta)$ correspond respectively to dimensionless velocity, pressure and temperature and are usually referred as the primal variable in the current setting. Parameter α is the spatially varying design variable field determined by the optimization algorithm. For the natural-dominated convection problem, we consider the following boundary conditions:

$$\begin{aligned}
&\mathbf{u} = 0, && \nabla p = 0, && \partial_n \theta = -1 && \text{on } \Gamma_1, \\
&\mathbf{u} = 0, && \nabla p = 0, && \partial_n \theta = 0 && \text{on } \Gamma_2, \\
&\mathbf{u} = u_i \mathbf{e}_y, && \nabla p = 0, && \theta = 0 && \text{on } \Gamma_i, \\
&\partial_n \mathbf{u} = 0, && p = 0, && \partial_n \theta = 0 && \text{on } \Gamma_o,
\end{aligned} \tag{2}$$

where ∂_n is the normal derivative defined as $\partial_n = n \cdot \nabla$.

3. Topology optimization formulation

The main goal of this paper is to deal with a multi-objective optimization problem in the asymmetrically heated channel, considering both pressure drop minimization described by a first objective function $\mathcal{J}_1$ and heat transfer maximization described by a second objective function $\mathcal{J}_2$. The optimization problem can then be stated as:

$$\begin{aligned} \text{minimize:} \quad & \mathcal{J}(\mathbf{u}, p, \theta) = \gamma_1\ \mathcal{J}_1(\mathbf{u}, p, \theta) + \gamma_2\ \mathcal{J}_2(\mathbf{u}, p, \theta), \\ \text{subject to:} \quad & \text{Governing equations (1)}, \\ & \text{Boundary conditions (2)}. \end{aligned} \tag{3}$$

where the cost function $\mathcal{J}$ is the combination of the two objectives functions, γ_1 and γ_2 are weighting coefficients. It is easy to observe that, for $\gamma_1 \gg \gamma_2$, the multi-objective function is directed to a minimum power dissipation problem, while for $\gamma_1 \ll \gamma_2$, a maximum heat dissipation problem arises.

3.1. Definition of the cost functions

As indicated by several authors [30, 12, 17, 14], cost functions $\mathcal{J}_1$ and $\mathcal{J}_2$ are often expressions of the work of forces or powers that one either wish to minimize or to maximize. A classical cost function used by Marck et al. [12], Othmer [19] for evaluating total pressure losses is :

$$f(\mathbf{u}, p) = \int_\Gamma -\mathbf{n} \cdot \mathbf{u}\ \left(p + \frac{1}{2}\ |\mathbf{u}|^2 \right) \mathrm{d}S. \tag{4}$$

Also, Marck et al. [12], Kontoleontos et al. [17] evaluate the thermal power by the next expression:

$$f(\mathbf{u}, \theta) = \int_\Gamma \mathbf{n} \cdot \mathbf{u}\ \theta\ \mathrm{d}S. \tag{5}$$

In our study, we propose to evaluate mechanical power and thermal power via two new expressions of both cost functions. As we will show below, these functions give an optimal design in less iteration number and do not require the use of filtering techniques. They will also allow to obtain a good connectivity between elements of solid regions. For a system with an inlet, an outlet, an average velocity and an average temperature, we define the thermal power as the product of the mass flow, the volume heat capacity and the difference of temperature between the entrance and the exit of the system. Likewise, mechanical power is defined as the product of mass flow rate and the difference of total pressure between the entrance and the exit of the system. In that way, we chose the work of pressure forces to minimize the power dissipated in the channel as used in systemic approach. Hence, the first cost function can be written as:

$$\begin{aligned}\mathcal{J}_1(\mathbf{u},p) = \; & -\frac{1}{|\Gamma_i|}\int_{\Gamma_i} p_t \;\mathrm{d}S \int_{\Gamma_i} \mathbf{u}\cdot\mathbf{n}\;\mathrm{d}S \\ & -\frac{1}{|\Gamma_o|}\int_{\Gamma_o} p_t \;\mathrm{d}S \int_{\Gamma_o} \mathbf{u}\cdot\mathbf{n}\;\mathrm{d}S,\end{aligned} \tag{6}$$

where $p_t = p + 1/2\ |\mathbf{u}|^2$ is the total pressure, Γ_i and Γ_o are respectively the entrance (inlet) and the exit (outlet) of the channel.

The second cost function concerns thermal exchange maximization and is given by:

$$\begin{aligned}\mathcal{J}_2(\mathbf{u},\theta) = \; & \frac{1}{|\Gamma_i|}\int_{\Gamma_i} \theta \;\mathrm{d}S \int_{\Gamma_i} \mathbf{u}\cdot\mathbf{n}\;\mathrm{d}S \\ & +\frac{1}{|\Gamma_o|}\int_{\Gamma_o} \theta \;\mathrm{d}S \int_{\Gamma_o} \mathbf{u}\cdot\mathbf{n}\;\mathrm{d}S.\end{aligned} \tag{7}$$

We can observe that this systemic approach for defining our cost functions enables to dissociate total pressure or temperature from the mass flow rate, since velocity profile is imposed at the entrance. Besides, minimizing (Eq. 7) is equivalent to minimize the mean temperature at apertures. On the contrary, minimizing (Eq. 5) is equivalent to minimize the bulk temperature which is defined as:

$$\theta_b = \frac{1}{\int_{\Gamma_i} \ \mathbf{u}\cdot\mathbf{n}\; d\Gamma} \int_{\Gamma_i} \theta\ \mathbf{u}\cdot\mathbf{n}\; d\Gamma. \tag{8}$$

One can finally remark that, our expression of thermal power consists in the mean temperature whereas expressions used by Marck et al. [12], Kontoleontos et al. [17] corresponds to the bulk temperature.

3.2. Multi-objective optimization

In multi-objective optimization, the challenge is to benefit from both objective functions. As introduced in previous subsection, the objective function based on maximization of thermal exchanges can involve the increase of pressure drop and conversely for the objective function relative to the dissipation of power. Before combining linearly the two functions, they must then be rescaled to have the same order of magnitude. This can be done by using an Aggregate Objective Function (AOF), also known as the weighted-sum approach, which is based on a linear combination of both objective functions [44, 45]. The latter reads:

$$\hat{f} = \frac{f - f_{min}}{f_{max} - f_{min}} \tag{9}$$

where f is either $\mathcal{J}_1$ or $\mathcal{J}_2$. As explained by Marck et al. [12], the other four parameters are determined by solving both optimization problems independently (3) for min $\mathcal{J}_1$ and max $\mathcal{J}_2$. Consequently, both rescaled objective functions are ranged between 0 and 1. Such a rescaling allows to consider the following linear combination:

$$\hat{\mathcal{J}} = \omega\ \hat{\mathcal{J}}_1 - (1 - \omega)\hat{\mathcal{J}}_2 \tag{10}$$

where $\omega \in [0, 1]$ is the weight balancing the influence of each objective function. Note that this combination involves the opposite of $\mathcal{J}_2$ since one aims at minimizing the combinatory function $\hat{\mathcal{J}}$. Thereafter, $\hat{\mathcal{J}}_1$ and $\hat{\mathcal{J}}_2$ are used only during the optimization process.

4. Topology optimization methods

Applying topology optimization to this problem aims to minimize an objective function $\mathcal{J}$ by finding an optimal distribution of solid and fluid element in the computational domain. The goal of topology optimization is to end up with binary designs, i.e avoid that the design variables take other value than those representing the fluid or the solid. This is usually carried out by penalizing the intermediate densities with respect to the material parameters, such as inverse permeability and effective diffusivity. A standard approach is to use interpolation functions. We are also going to use gradient-based algorithm that relies on the continuous adjoint method.

4.1. Interpolation functions

The additional term $h_\tau(\alpha)$ in (Eq. 1) physically corresponds to the ratio of a kinematic viscosity and a permeability. As proposed by Guest et al. [46], Sigmund [32], Zhao et al. [47], a projection approach is employed to relate the element-based design variables to the physical densities firstly and to the thermal diffusivity, secondly. We defined two smooth regularization of Heaviside functions for these interpolations. The interpolation function for the thermal diffusivity of each element is $k_\tau(\alpha)$, both functions were defined in Ramalingom et al. [24] where it is shown that the intermediate zones can be as small as wanted. Regions with very high permeability can be considered as solid regions, and those with low permeability regions are interpreted as pure fluid.

Inverse permeability is thus interpolated with the following formula

$$h_\tau(\alpha) = \alpha_{max} \left(\frac{1}{1 + \exp\left(-\tau(\alpha - \alpha_0)\right)} - \frac{1}{1 + \exp\left(\tau\alpha_0\right)} \right), \tag{11}$$

where α_0 is the abscissa slope of the sigmoid function, α_{max} is the maximum value that the design parameter α can take and is set to 2 10^5. In the present study, we chose $\alpha_0 = 20$ and $\alpha \in [0, \alpha_{max}]$.

The difference in the adimensional thermal diffusivities of the fluid and solid regions in considered through the interpolation of effective diffusivity k_τ as follows:

$$k_\tau(\alpha) = \frac{1}{k_f} \left[k_f + (k_s - k_f) \left(\frac{1}{1 + \exp\left(-\tau(\alpha - \alpha_0)\right)} - \frac{1}{1 + \exp\left(\tau\alpha_0\right)} \right) \right], \tag{12}$$

where k_s and k_f are respectively the thermal diffusivity of solid domains and the thermal diffusivity of the fluid domains.

4.2. Adjoint problem

The Lagrange multiplier method [48] is used to get an optimization problem without constraints and can be used to get the sensitivity of the cost function $\mathcal{J}$. The Lagrangian is defined as

$$\begin{aligned} &\mathcal{L}(\mathbf{u}, p, \theta, \mathbf{u}^*, p^*, \theta^*, \alpha) = \mathcal{J}(\mathbf{u}, p, \theta) \\ &+ \int_\Omega \mathcal{R}(\mathbf{u}, p, \theta) \cdot (\mathbf{u}^*, p^*, \theta^*) d\Omega, \end{aligned} \tag{13}$$

where $(\mathbf{u}^*, p^*, \theta^*)$ are the adjoint variables and $\mathcal{R}(\mathbf{u}, p, \theta) = 0$ corresponds to the governing equations (1). The critical points of $\mathcal{L}$ with respect to the adjoint variables give the constraint of the optimization problem (3) while the critical point with respect to the primal variable yield the so-called adjoint problem. The latter can be derived as in Othmer [19] (see also [24]) and is given by

$$\begin{aligned} \nabla p^* - h_\tau(\alpha)\mathbf{u}^* + \theta\ \nabla\theta^* + \ Re^{-1}\Delta\mathbf{u}^* + \nabla\mathbf{u}^*\ \mathbf{u} - (\mathbf{u}^*\cdot\nabla)\mathbf{u} &= 0 \quad \text{in} \quad \Omega, \\ \nabla\cdot\mathbf{u}^* &= 0 \quad \text{in} \quad \Omega, \\ Ri\ \mathbf{u}^*\cdot\overrightarrow{e_y} + \mathbf{u}\cdot\nabla\theta^* + \nabla\cdot(Re^{-1}Pr^{-1}k_\tau(\alpha)\nabla\theta^*) &= 0 \quad \text{in} \quad \Omega, \end{aligned} \tag{14}$$

together with the boundary conditions

$$\begin{aligned} &\mathbf{u}^* = 0,\ \partial_n\theta^* = 0,\ \partial_n p^* = 0 && \text{on } \Gamma_1\cup\Gamma_2, \\ &u_t^* = 0,\ \theta^* = 0,\ \frac{\partial\mathcal{J}}{\partial p} = -u_n^*,\ \partial_n p^* = 0 && \text{on } \Gamma_i, \\ &u_t^* = 0,\ \frac{\partial\mathcal{J}}{\partial\theta} = -\theta^*\ u_n - Re^{-1}Pr^{-1}k_\tau(\alpha)\partial_n\theta^* && \text{on } \Gamma_o, \\ &\frac{\partial\mathcal{J}}{\partial\mathbf{u}}\cdot\mathbf{n} = -p^* - \theta^*\ \theta - Re^{-1}\ \partial_n\mathbf{u}^*\cdot\mathbf{n} - u_n^*\ u_n - \mathbf{u}\cdot\mathbf{u}^* && \text{on } \Gamma_o, \end{aligned} \tag{15}$$

where $u_n = \mathbf{u}\cdot\mathbf{n}$ and the derivatives of $\mathcal{J}$ defined in (3) with respect to $(\mathbf{u},\ p,\ \theta)$ are given by

$$\begin{aligned} \left.\frac{\partial\mathcal{J}}{\partial p}\right|_{\Gamma_i} &= -\gamma_1\ \frac{1}{|\Gamma_i|}\int_{\Gamma_i}\mathbf{u}\cdot\mathbf{n}\ \mathrm{d}S \\ \left.\frac{\partial\mathcal{J}}{\partial\theta}\right|_{\Gamma_o} &= \ \ \gamma_2\ \frac{1}{|\Gamma_o|}\int_{\Gamma_o}\mathbf{u}\cdot\mathbf{n}\ \mathrm{d}S \\ \left.\frac{\partial\mathcal{J}}{\partial\mathbf{u}}\right|_{\Gamma_o} &= -\gamma_1\ \frac{1}{|\Gamma_o|}\mathbf{n}\int_{\Gamma_o}p_t\ \mathrm{d}S - \gamma_1\ \mathbf{u}\cdot\int_{\Gamma_o}\mathbf{u}\cdot\mathbf{n}\ \mathrm{d}S \\ &\quad +\ \gamma_2\ \frac{1}{|\Gamma_o|}\mathbf{n}\int_{\Gamma_o}\theta\ dS. \end{aligned} \tag{16}$$

We emphasize that the adjoint problem (14,15) has been derived for the cost function $\mathcal{J}$ given by (3). Nevertheless, in the numerical result, we wish to minimize the rescaled cost function $\hat{\mathcal{J}}$ whose derivatives with respect to

$(\mathbf{u},\ p,\ \theta)$ are obtained thanks to (16) with

$$\gamma_1 = \frac{\omega}{\mathcal{J}_{1,max} - \mathcal{J}_{1,min}},\ \gamma_2 = \frac{-(1-\omega)}{\mathcal{J}_{2,max} - \mathcal{J}_{2,min}}.$$

4.3. Implementation

Topology optimization problem is solved by iterative calculations as carried out by Ramalingom et al. [24]. The main steps of the algorithm for the topology optimization are summarized in Table 2. They consist to compute sensitivities by adjoint method and evaluate the optimality condition. If a stopping criterion is met, the computations are terminated. For our simulations, we used $\epsilon = 10^{-7}$. The forward problem (1) and the adjoint problem (14) are implemented using OpenFOAM [49]. The generalized Geometric-Algebraic Multi-Grid (GAMG) solver with a cell-centered colocalized finite volume approach is used. In Step 5, the design variables are evaluated by using the conjugated-gradient descent direction method associated to Polack-Ribiere method $\beta^{PR}_{k+1} = \frac{\nabla\mathcal{J}^T_{k+1}\ (\nabla\mathcal{J}_{k+1} - \nabla\mathcal{J}_k)}{\nabla\mathcal{J}^T_k\ \nabla\mathcal{J}_k}$. The optimality condition is given by the critical point of the Lagrangian with respect to the design parameter α as follows:

$$\begin{aligned} &\frac{\partial h_\tau}{\partial\alpha}\,\mathbf{u}\cdot\mathbf{u}^* + \frac{\partial k_\tau}{\partial\alpha}\nabla\theta\cdot\nabla\theta^* = 0 \quad &&\text{in } \Omega, \\ &\frac{\partial k_\tau}{\partial\alpha}\,\theta^* = 0 \ \text{ with } \partial_n\theta = -1 &&\text{on } \Gamma_1. \end{aligned} \tag{17}$$

5. Results

First of all, it is important to note that the problem is purely academic and the values of various parameters as Prandtl number set to 0.71 corresponding

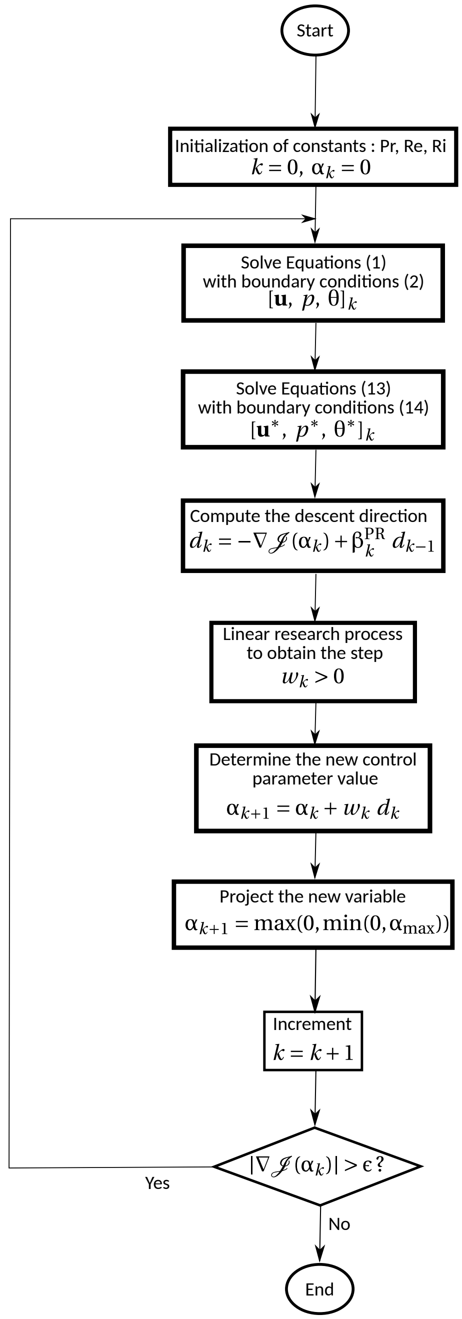

Figure 2: Algorithm used to solve the topology optimization (3)

to a fluid/liquid, and k_s/k_f have been therefore set to 3. As they are in the range of realistic problems, they are thought to be representative of the problems that can be physically encountered. The problem is investigated for $\mathrm{Ri} = \{100, 200, 400\}$ under constant $\mathrm{Re} = 400$ which is equivalent to increase the dominance of natural convection in the conducto-convection problem. These values have been chosen in accordance with the study of Li et al. [50] on reversal flows in the asymmetrically heated channel. We chose $\alpha_0 = 20$ and set α_{max} to $2 \cdot 10^{\ 5}$, keeping in mind that similar results have been obtained for $\alpha_{max} = 10^{\ 6}$. A vertical velocity profile at the entrance of the channel is considered in accordance with the value of $\mathrm{Re} = 400$. Its profile is defined by the following equation:

$$u_i(x) = -\ 6.1\ x^2 + 6.1\ x.$$

For this study, we chose different values of ω in line with the importance given to the different cost functions $\mathcal{J}_1$ or $\mathcal{J}_2$. All results performed in this paper correspond to the thermal and mechanical powers defined as $\mathcal{J}_1$ and $\mathcal{J}_2$. Moreover, in order to be sure that no material is added at the entrance of the channel during the optimization process, we solved the problem by imposing fluid domain at the lower part of the channel, i.e. $\alpha = 0$ for the element in $[0, 1] \times [0, 1]$. We compare first the various optimized designs obtained and the structure of the flow in new designs. For each value of Richardson number, we compute the proportion Q_t of material added in the domain Ω as follows:

$$Q_t = \frac{\int_\Omega h_\tau(\alpha)\ d\Omega}{\alpha_{max}\ V_{tot}},\ \text{where } V_{tot} \text{ is the total volume of } \Omega. \tag{18}$$

In order to demonstrate the increase of heat transfer after optimization, we compute the inverse of the difference between the temperature at the left wall and the bulk temperature, i.e the Nusselt number defined in Desrayaud et al. [42] by:

$$
\begin{aligned}
Nu_2(y) &= \frac{1}{\theta(0,y)-\theta_{bulk}(y)} \\
\text{where } \theta_{bulk}(y) &= \frac{1}{q_{in}(y=0)}\ \int_0^1 u(x,y)\ \theta(x,y)\ dx,
\end{aligned}
\tag{19}
$$

$y = 3H/2$ corresponds to the end of the heated plate and q_{in} is the mass flow rate entering the channel at $y = 0$.

In a second time, we compare our results obtained for Ri=100 to those obtained with objectives function usually used in literature, i.e. $\mathcal{J}_1$ and $\mathcal{J}_2$ are defined by (Eq. 4) and (Eq. 5).

5.1. Varying Richardson number

Figure 3 shows that the obtained designs at varying Ri differ from one to another, which is to be expected. When the natural convection forces become more dominant, the optimization algorithm adds more material in the channel. The proportion of material added in the vertical channel varies from 4.9% to 52.2%. So, the quantity of material increases when Richardson number increases. The structure of the flow in the channel is also modified. From Figure 3c, it can be seen that for Ri = 400, all of the material is kept close to the right wall of the domain and the flow circulation is obliged to be near the heated wall. This contributes to the second objective function corresponding to increase the thermal exchanges in the channel. Table 1 gives the Nusselt number at the exit of the heated plate for each Richardson number. Without optimization and whichever the Richardson number in the range considered, Nusselt number at the exit of hot plate is equal to 10.51 and the bulk temperature to 0.07. After optimization, Nusselt number varies from 11.86 to 15.06. Hence, we obtained a rise between 12.8% and 43.3%. So, Nusselt number is more important in the optimized design and it increases when Richardson number increases. Hence, we successfully increase thermal exchanges in the channel.

It can also be observed that the reversal flow is suppressed after optimization process. Indeed, material added by the algorithm at the end of the channel prevent the fluid from re-entering in the channel. As can be seen on Figure 5, vertical component of the velocity has a positive value in the channel after optimization and is null or very small in the solid region, as expected. That means our interpolation function gives an optimized design with no physical error as a non-null velocity in the solid regions without connectivity (Kreissl and Maute [51] and Lee [30]). Moreover, value of vertical component of the velocity increases when Ri increases (cf. Figure 4). That is due to the reduction of the section for the flow circulation which causes an acceleration of the fluid in the channel. The width of flow circulation after optimization for the case $\mathrm{Ri} = 100, \omega = 0.5$ is referenced on Figure 6, for example. This graph also demonstrates that the sigmoid function $h_\tau(\alpha)$ which interpolates the design variable α affects correctly volume elements to solid domains in order to avoid checkerboards. That brings to a well definition of the fluid-solid boundaries as obtained by Ramalingom et al. [24].

With regards of cost functions computation, our algorithm reduces the value of $\hat{\tilde{J}}$ over iterations as can be seen on Figure 7 for the case $Ri = 100$.

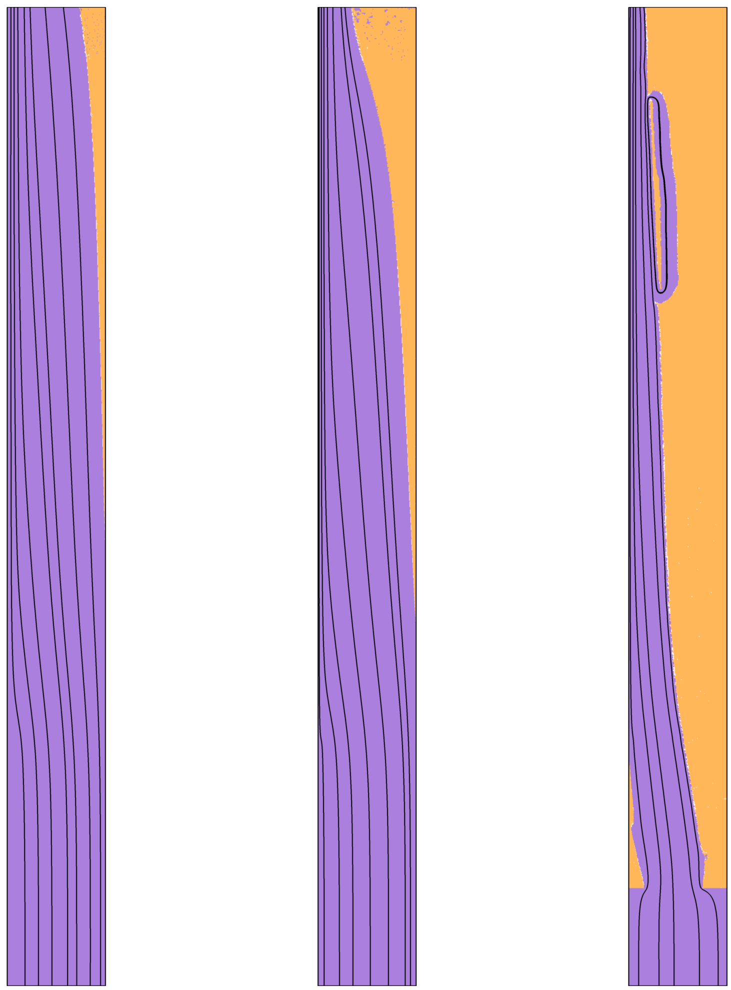

(a) Ri = 100
Q_t = 4.9%

(b) Ri = 200
Q_t = 13.3%

(c) Ri = 400
Q_t = 52.2%

Figure 3: Optimized designs and streamtraces at various Ri. Orange corresponds to solid material and purple corresponds to the fluid domain.

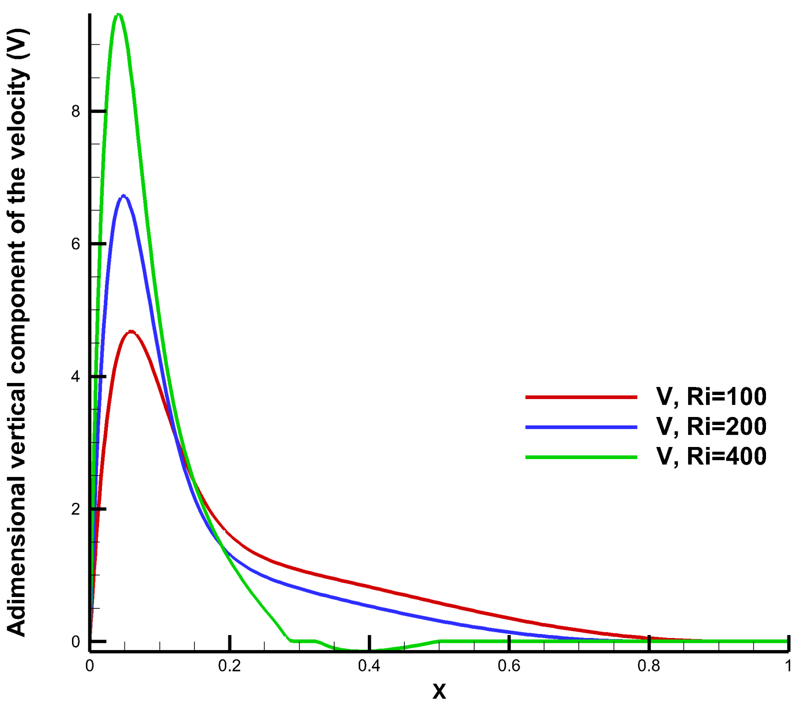

Figure 4: Adimensional vertical component of the velocity at the end of the hot plate of the channel $y = 3H/2$

Table 2 highlights the influence of Ri on thermal power and mechanical power. Indeed, as the Richardson number increases, the power due to work forces decreases and the thermal power in the channel increases. $\mathcal{J}_1$ is reduced by a factor 1.64 and $\mathcal{J}_2$ is reduced by a factor 1.51 (Table 2) for Ri = 100. When we compare $\mathcal{J}_1$ to its value without optimization $\mathcal{J}_1$Ref, we notice that sometimes the optimization algorithm added material which contributes to rising friction forces and pressure losses as long as the heat dissipation increases. Hence, for the case Ri = 200, $\mathcal{J}_1$ is reduced by a factor 1.13

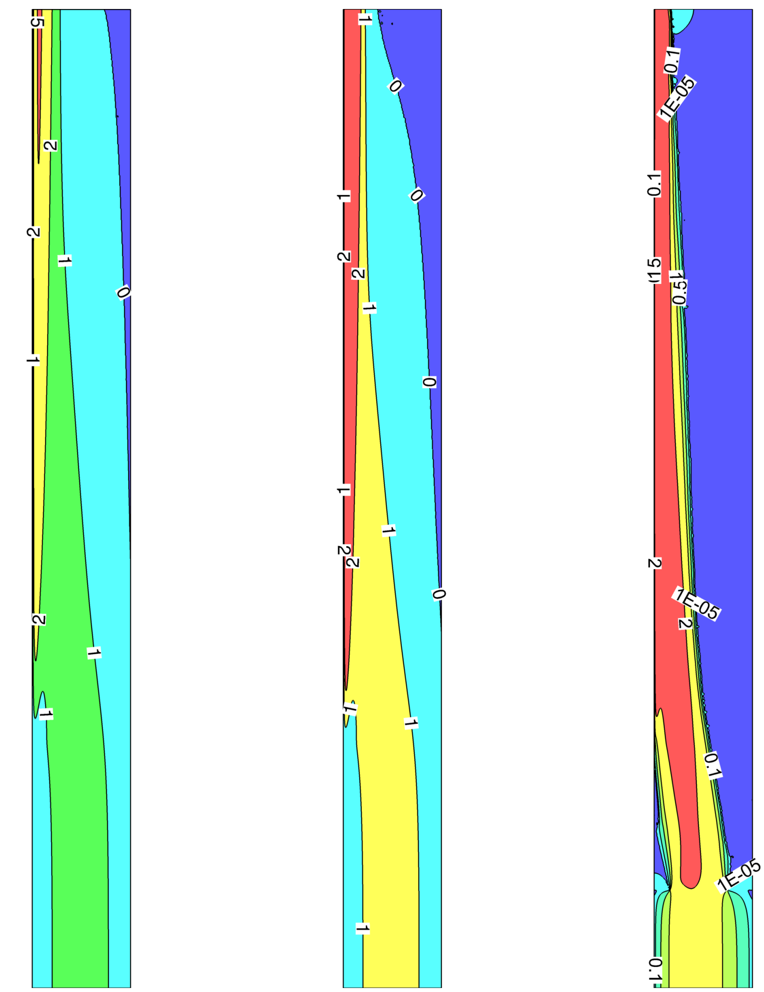

(a) Ri = 100 $\omega = 0.5$

(b) Ri = 200 $\omega = 0.85$

(c) Ri = 400 $\omega = 0.15$

Figure 5: Adimensional vertical velocity field at various Ri

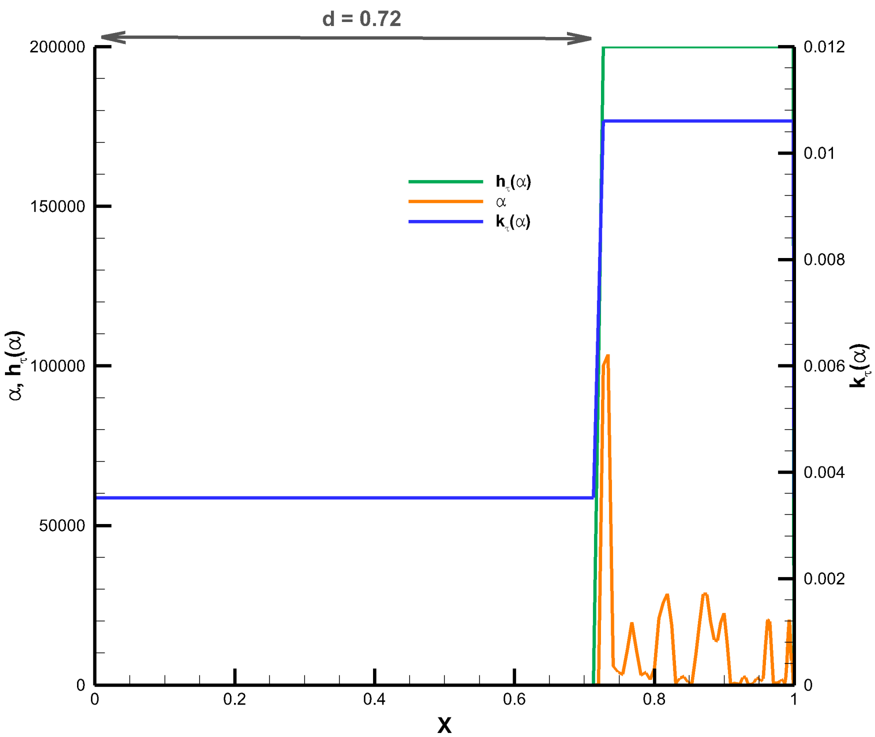

Figure 6: α, $h_\tau(\alpha)$ and $k_\tau(\alpha)$ at the end section of the channel for $\mathrm{Ri} = 100$ - annotation d is used for the width of the flow section

while $\mathcal{J}_2$ is increased by a factor 0.46. On the contrary, for the case $\mathrm{Ri} = 400$, $\mathcal{J}_1$ is increased by a factor 0.26 while $\mathcal{J}_2$ is reduced by a factor 0.64. These cases illustrated that our algorithm enables to add material in the channel in order to contribute to one or other cost functions according to the weighted coefficient ω. Hence, for the case $\mathrm{Ri} = 200$, we chose to prioritize the minimization of mechanical power with $\omega = 0.85$. For the case $\mathrm{Ri} = 400$, we chose to prioritize the maximization of heat transfer with $\omega = 0.15$. We can conclude that the algorithm succeeds to minimize/maximize one or other

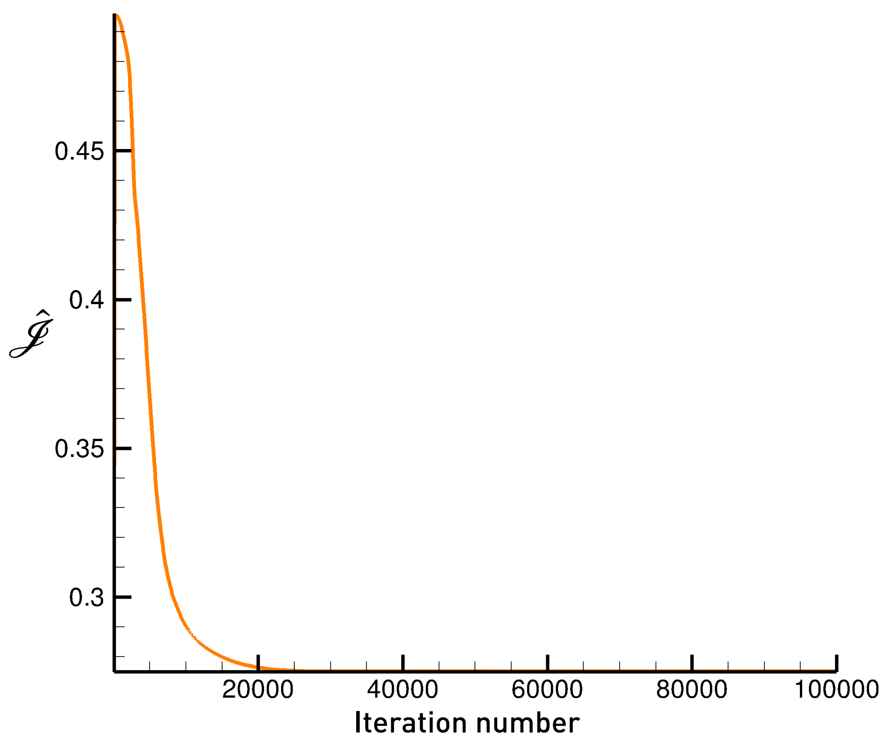

Figure 7: Evolution of $\hat{\mathcal{J}}$ over iterations - Ri $= 100, \omega = 0.5$

cost functions by adding material without penalizing too much the other.

5.2. Comparison with classical functions of literature (Eq. 4) and (Eq. 5)

In this section, we compare optimization results obtained with our cost functions to those obtained with classical cost functions referenced in the literature, i.e those defined by (Eq. 4) and (Eq. 5). First of all, Figure 11 shows different snapshot of optimized designs obtained over iterations with classical cost functions (4) and (5). We stop the computation at iteration number 187500. We notice that our algorithm has a tendency to fill up the

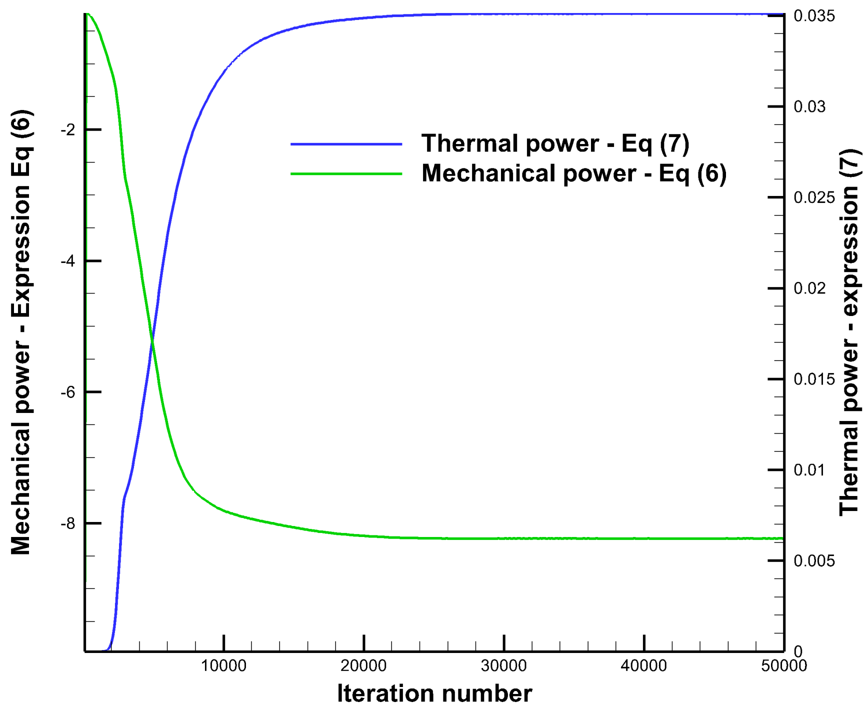

Figure 8: Evolution of thermal power and mechanical power over iterations - $\mathrm{Ri} = 100, \omega = 0.5$

channel with material before suppresses it in order to achieve the goal defined by the classical cost functions. In the same way, Figure 9 shows different snapshots of optimized designs over iterations with the objective functions that we propose in this paper. We obtain the final optimized design at iteration number 84000, which is faster compared to the previous simulation. Ramalingom et al. [24] have used the same algorithm with the classical cost functions to deal with cases where Ri= 2.8. When Richardson number is more important (set to 100), the various designs obtained over iterations with these

	θ_{bulk}	$Nu_2(3H/2)$
$Ri = 100$	0.027	11.86
$Ri = 200$	0.034	12.99
$Ri = 400$	0.039	15.06

Table 1: Nusselt number and adimensional bulk temperature at the end of the hot plate for various Richardson numbers

	Ri = 100	Ri = 200	Ri = 400
$\mathcal{J}_1\text{ref}/\mathcal{J}_1$	1.64	1.13	0.26
$\mathcal{J}_2\text{ref}/\mathcal{J}_2$	1.51	0.46	0.64

Table 2: Reduction factor of cost functions - ref corresponds to the value of cost functions without optimization

classical cost functions demonstrate that they are not appropriate to deal with heat transfer problem dominated by natural convection. Cost functions that dissociate pressure and temperature to the mass flow rate by considering average quantities essentially give stable optimized results. Moreover, we observe that the algorithm adds material just at the right plate on the top, this strategy is sufficient to prevent the fluid from re-entering at the top-end of the channel. Second, the channel is filled up at 45.03% with classical cost functions, while it is filled up at 4.9% with our cost functions. So, the new expressions of mechanical and thermal power give optimized designs with less material. Finally, when we enlarge the top end of the optimized designs and we compare both in Figure 10, we can see that the new expressions of objective functions allow a best connectivity between solid elements. No

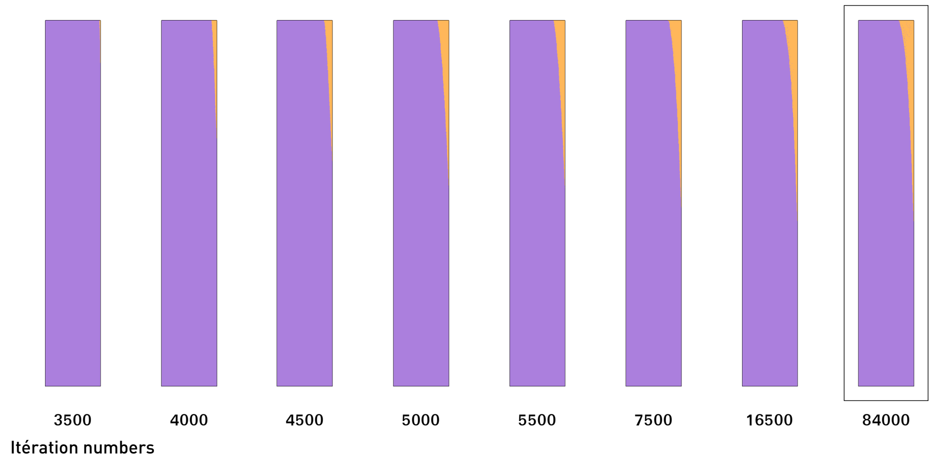

Figure 9: Designs obtained over iterations with functional objectives defined in this paper

isolated material is added in the channel as encountered by some authors [41, 15, 12, 13] in the literature. Hence, that contributes to diminishing the first objective function, i.e pressure losses in the channel. So, for this configuration case of the channel, i.e. where the fluid flow moves essentially by natural convection, the classical cost functions of the literature seem to be inappropriate. With our new expressions of mechanical and thermal power, we obtain an optimized design in less time of computation and with less quantity of material. Moreover, connectivity in solid region is better.

6. Conclusion

An optimization problem considering both pressure drop minimization and heat transfer maximization in the asymmetrically heated channel has been examined. The problem is handled in natural convection with several values of Richardson number taken in $\{100, 200, 400\}$. First of all, two objective functions are investigated representing the work of forces for the

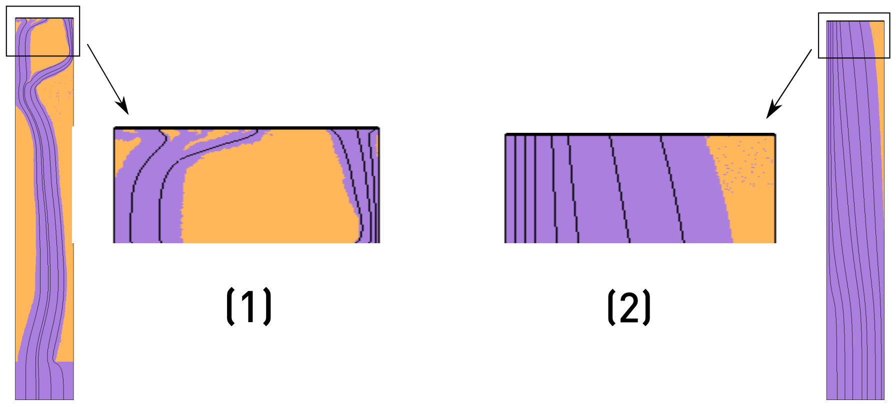

Figure 10: Comparison of solid regions at the end of the channel for classical cost functions of literature (1) and cost functions in this paper (2)

mechanical power and heat exchanges with the thermal power. In accordance with the physical problem considered, a weighted coefficient is chosen for the combined cost function. These functions allow to obtain optimal designs and they are relatively reduced in accordance with the weight affected to each of them. For Richardson number equal to 100, optimization results obtained with cost functions proposed in this paper are compared to those obtained with cost functions classically used in the literature. Several conclusions have been drawn. First of all, the reversal flow in the channel is suppressed at the end of the optimization. That contributes to reducing pressure losses in the channel. Then, the new expressions of cost functions avoid the use of filter techniques as no checkerboards pattern are observed. The values of cost functions converge asymptotically over iterations with the new expressions of mechanical and thermal powers, contrarily to those used in the literature. This approach that consists of dissociating quantities in the expression of cost functions by considering average quantities is well adapted to natu-

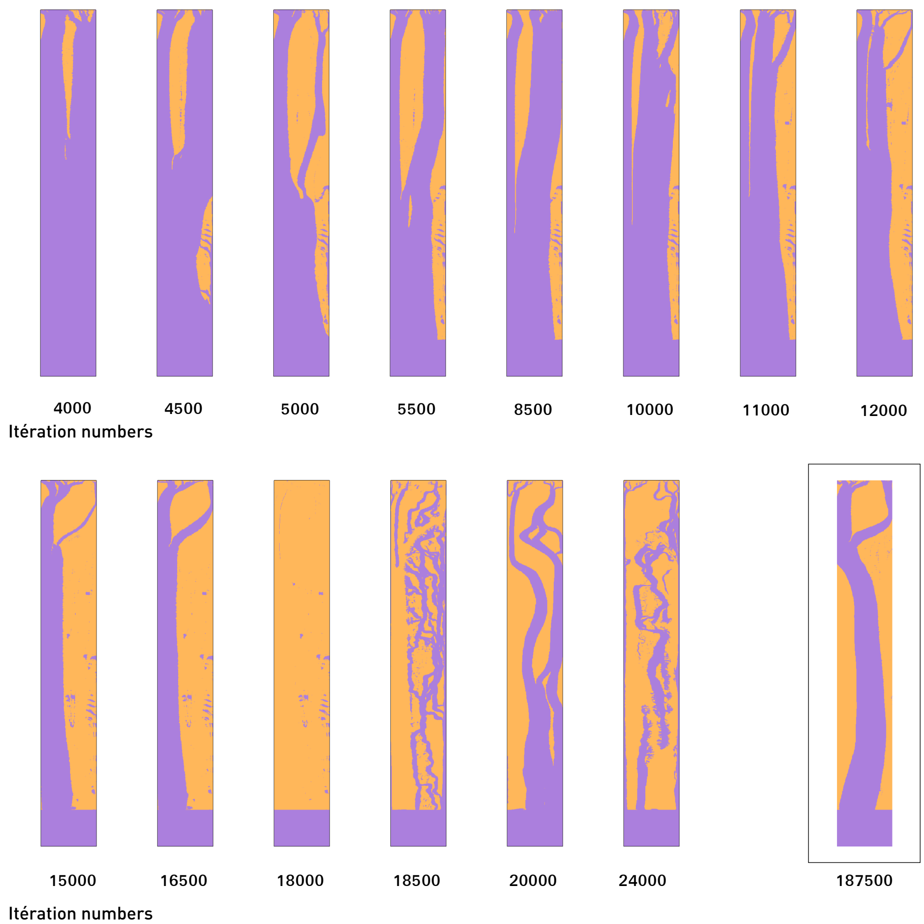

Figure 11: Designs obtained over iterations with cost functions defined in this paper

ral convection phenomena. Moreover, the obtained designs with these new costs functions show a better connectivity in the solid region, contrarily to the design obtained with classical cost functions. Concerning the fluid-solid boundary, they are well-defined during the optimization process thanks to two sigmoid functions used for the interpolation of both the design variable and the effective diffusivity. Finally, the optimization algorithm is able to increase thermal exchanges while maintaining the pressure losses due to friction, thanks to the combined objective functions used. Thermal exchanges are evaluated by the calculation of Nusselt number based on the bulk temperature. They are more important with the obtained optimized designs and increase with Richardson number values. In conclusion, this study highlights the importance of the expression of cost functions in a topology optimization problem, dominated by natural convection forces. The influence of the Richardson is observed on the quantity of material added in the optimized channel. As future work, we suggest a more complete heat and mass transfer model might be considered, as pure natural convection problems and radiation problems.

Acknowledgements

Computations have been performed on the University of Reunion Island supercomputer facility.

References

[1] M. P. Bendsøe, N. Kikuchi, Generating optimal topologies in structural design using a homogenization method, Computer methods in applied mechanics and engineering 71 (2) (1988) 197–224.

[2] O. Sigmund, K. Maute, Topology optimization approaches, 2013.

[3] H. A. Eschenauer, N. Olhoff, Topology optimization of continuum structures: a review, Applied Mechanics Reviews 54 (4) (2001) 331–390.

[4] Q. Q. Liang, Performance-based optimization: a review, Advances in Structural Engineering 10 (6) (2007) 739–753.

[5] B. Hassani, E. Hinton, A review of homogenization and topology opimization IIanalytical and numerical solution of homogenization equations, Computers & structures 69 (6) (1998) 719–738.

[6] B. Hassani, E. Hinton, A review of homogenization and topology optimization Ihomogenization theory for media with periodic structure, Computers & Structures 69 (6) (1998) 707–717.

[7] B. Hassani, E. Hinton, A review of homogenization and topology optimization IIItopology optimization using optimality criteria, Computers & structures 69 (6) (1998) 739–756.

[8] M. Y. Wang, X. Wang, D. Guo, A level set method for structural topology optimization, Computer methods in applied mechanics and engineering 192 (1-2) (2003) 227–246.

[9] T. Borrvall, J. Petersson, Topology optimization of fluids in Stokes flow, International journal for numerical methods in fluids 41 (1) (2003) 77–107.

[10] T. Dbouk, A review about the engineering design of optimal heat transfer systems using topology optimization, Applied Thermal Engineering 112 (2017) 841–854.

[11] C. Othmer, Adjoint methods for car aerodynamics, Journal of Mathematics in Industry 4 (1) (2014) 6.

[12] G. Marck, M. Nemer, J.-L. Harion, Topology optimization of heat and mass transfer problems: laminar flow, Numerical Heat Transfer, Part B: Fundamentals 63 (6) (2013) 508–539.

[13] J. Alexandersen, N. Aage, C. S. Andreasen, O. Sigmund, Topology optimisation for natural convection problems, International Journal for Numerical Methods in Fluids 76 (10) (2014) 699–721.

[14] A. A. Koga, E. C. C. Lopes, H. F. V. Nova, C. R. de Lima, E. C. N. Silva, Development of heat sink device by using topology optimization, International Journal of Heat and Mass Transfer 64 (2013) 759–772.

[15] T. E. Bruns, Topology optimization of convection-dominated, steady-state heat transfer problems, International Journal of Heat and Mass Transfer 50 (15-16) (2007) 2859–2873.

[16] G. H. Yoon, Topological design of heat dissipating structure with forced convective heat transfer, Journal of Mechanical Science and Technology 24 (6) (2010) 1225–1233.

[17] E. Kontoleontos, E. Papoutsis-Kiachagias, A. Zymaris, D. Papadimitriou, K. Giannakoglou, Adjoint-based constrained topology optimization for viscous flows, including heat transfer, Engineering Optimization 45 (8) (2013) 941–961.

[18] E. M. Papoutsis-Kiachagias, K. C. Giannakoglou, Continuous adjoint methods for turbulent flows, applied to shape and topology optimization: Industrial applications, Archives of Computational Methods in Engineering 23 (2) (2016) 255–299.

[19] C. Othmer, A continuous adjoint formulation for the computation of topological and surface sensitivities of ducted flows, International Journal for Numerical Methods in Fluids 58 (8) (2008) 861–877.

[20] A. Bastide, P.-H. Cocquet, D. Ramalingom, Penalization model for navier-stokes-darcy equation with application to porosity-oriented topology optimization, Mathematical Models and Methods in Applied Sciences 0 (0) (2017) 1–32.

[21] Z.-X. Tong, M.-J. Li, J.-J. Yan, W.-Q. Tao, Optimizing thermal conductivity distribution for heat conduction problems with different optimization objectives, International Journal of Heat and Mass Transfer 119 (2018) 343–354.

[22] C. Othmer, T. Kaminski, R. Giering, Computation of topological sensitivities in fluid dynamics: cost function versatility, in: ECCOMAS CFD 2006: Proceedings of the European Conference on Computational Fluid Dynamics, Egmond aan Zee, The Netherlands, September 5-8, 2006, Citeseer, 1–12, 2006.

[23] M. Zhou, G. Rozvany, The COC algorithm, Part II: topological, geometrical and generalized shape optimization, Computer Methods in Applied Mechanics and Engineering 89 (1-3) (1991) 309–336.

[24] D. Ramalingom, P.-H. Cocquet, A. Bastide, A new interpolation technique to deal with fluid-porous media interfaces for topology optimization of heat transfer, Computers & Fluids 168 (2017) 144 – 158.

[25] F. M. White, Fluid Mechanics Fourth Edition, 2017.

[26] T. L. Bergman, F. P. Incropera, A. S. Lavine, D. P. DeWitt, Introduction to heat transfer, John Wiley & Sons, 2011.

[27] P. Coffin, K. Maute, Level set topology optimization of cooling and heating devices using a simplified convection model, Structural and multidisciplinary optimization 53 (5) (2016) 985–1003.

[28] B. S. Lazarov, O. Sigmund, Filters in topology optimization based on Helmholtz-type differential equations, International Journal for Numerical Methods in Engineering 86 (6) (2011) 765–781.

[29] T. Bruns, A reevaluation of the SIMP method with filtering and an alternative formulation for solid–void topology optimization, Structural and Multidisciplinary Optimization 30 (6) (2005) 428–436.

[30] K. Lee, Topology optimization of convective cooling system designs, Ph.D. thesis, University of Michigan, 2012.

[31] J. Alexandersen, C. S. Andreasen, N. Aage, B. S. Lazarov, O. Sigmund, Topology optimisation for coupled convection problems, in: 10th world Congress on structural and multidisciplinary optimization, Orlando, 19–24, 2013.

[32] O. Sigmund, Morphology-based black and white filters for topology optimization, Structural and Multidisciplinary Optimization 33 (4-5) (2007) 401–424.

[33] E. Bacharoudis, M. G. Vrachopoulos, M. K. Koukou, D. Margaris, A. E. Filios, S. A. Mavrommatis, Study of the natural convection phenomena inside a wall solar chimney with one wall adiabatic and one wall under a heat flux, Applied Thermal Engineering 27 (13) (2007) 2266–2275.

[34] F. Incropera, Convection heat transfer in electronic equipment cooling, Journal of heat transfer 110 (4b) (1988) 1097–1111.

[35] R. B. Yedder, E. Bilgen, Natural convection and conduction in Trombe wall systems, International Journal of Heat and Mass Transfer 34 (4-5) (1991) 1237–1248.

[36] B. F. Balunov, A. Babykin, R. A. Rybin, V. A. Krylov, V. N. Tanchuk, S. A. Grigor'ev, Heat transfer at mixed convection in vertical and inclined flat channels of the vacuum chamber of the iter international thermonuclear reactor, High temperature 42 (1) (2004) 126–133.

[37] R. C. Martinelli, L. M. K. Boelter, The Analytical Prediction of Superposed Free and Forced Viscous Convection in a Vertical Pipe, by RC Martinelli and LMK Boelter..., University of California Press, 1942.

[38] J. Jackson, M. Cotton, B. Axcell, Studies of mixed convection in vertical tubes, International journal of heat and fluid flow 10 (1) (1989) 2–15.

[39] J. Bodoia, J. Osterle, The development of free convection between heated vertical plates, Journal of Heat Transfer 84 (1) (1962) 40–43.

[40] W. Elenbaas, Heat dissipation of parallel plates by free convection, Physica 9 (1) (1942) 1–28.

[41] G. Ho Yoon, Y. Young Kim, The element connectivity parameterization formulation for the topology design optimization of multiphysics systems, International journal for numerical methods in engineering 64 (12) (2005) 1649–1677.

[42] G. Desrayaud, E. Chénier, A. Joulin, A. Bastide, B. Brangeon, J. Caltagirone, Y. Cherif, R. Eymard, C. Garnier, S. Giroux-Julien, et al., Benchmark solutions for natural convection flows in vertical channels submitted to different open boundary conditions, International journal of thermal sciences 72 (2013) 18–33.

[43] D. Ramalingom, P.-H. Cocquet, A. Bastide, Numerical study of natural convection in asymmetrically heated channel considering thermal stratification and surface radiation, Numerical Heat Transfer, Part A: Applications 72 (9) (2017) 681–696.

[44] T. W. Athan, P. Y. Papalambros, A note on weighted criteria methods for compromise solutions in multi-objective optimization, 1996.

[45] A. Messac, C. Puemi-Sukam, E. Melachrinoudis, Aggregate objective functions and Pareto frontiers: required relationships and practical implications, Optimization and Engineering 1 (2) (2000) 171–188.

[46] J. K. Guest, J. H. Prévost, T. Belytschko, Achieving minimum length scale in topology optimization using nodal design variables and projection functions, International journal for numerical methods in engineering 61 (2) (2004) 238–254.

[47] X. Zhao, M. Zhou, O. Sigmund, C. S. Andreasen, A poor mans approach to topology optimization of cooling channels based on a Darcy flow model, International Journal of Heat and Mass Transfer 116 (2018) 1108–1123.

[48] H. Everett III, Generalized Lagrange multiplier method for solving problems of optimum allocation of resources, Operations research 11 (3) (1963) 399–417, ISSN 0030-364X.

[49] G. H. W. Et al., A tensorial approach to computational continuum mechanics using object- oriented techniques, Computers in physics 12.6 (1998) 620–631.

[50] R. Li, M. Bousetta, E. Chénier, G. Lauriat, Effect of surface radiation on natural convective flows and onset of flow reversal in asymmetrically heated vertical channels, International journal of thermal sciences 65 (2013) 9–27.

[51] S. Kreissl, K. Maute, Levelset based fluid topology optimization using the extended finite element method, Structural and Multidisciplinary Optimization 46 (3) (2012) 311–326.